

Energy Dissipation of RC Interior Beam-column Connection Confined by Lateral Reinforcements, Axial Force, and Column Longitudinal Reinforcements

Seitaro Tajiri & Hiroshi Fukuyama

Building Research Institute, Japan



15 WCEE
LISBOA 2012

Haruhiko Suwada

National Institute for Land and Infrastructure Management, Japan

Fumio Kusuhara & Hitoshi Shiohara

The University of Tokyo, Japan

SUMMARY:

This study investigates the energy dissipation capacity of reinforced concrete interior beam-column connections. Seven half-scale beam-column subassemblages whose joint expansion was confined by joint hoops, column axial load, and column longitudinal bars were tested under static cyclic loading. Based on the experimental results, the following conclusions were drawn: 1) Specimens confined by column axial load showed a higher energy dissipation capacity than the unconfined specimens; 2) The amount and yield strength of the joint hoops and column longitudinal bars had little effect on the energy dissipation capacity; and 3) The specimen with improved bond resistance showed a slightly higher energy dissipation capacity, but not as much as the specimens confined by column axial load.

Keywords: *Beam-column joint, Energy dissipation, Expansion constraint, Bond resistance, Reinforced concrete*

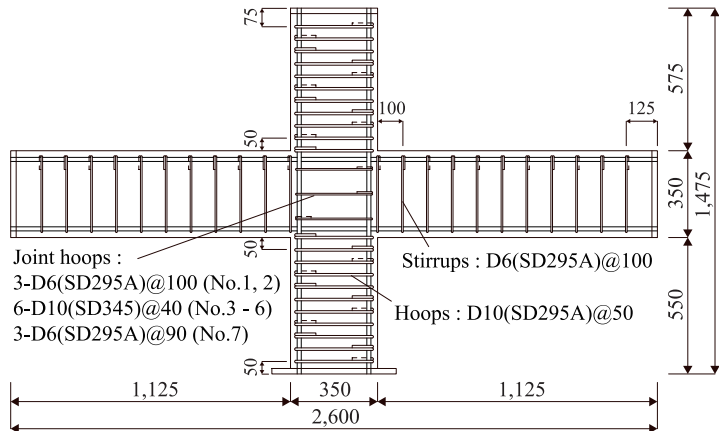
1. INTRODUCTION

In the structural design for earthquake resistance based on the inelastic displacement concept of reinforced concrete (RC) buildings, the energy dissipation which arises with the inelastic deformation of the whole structure is considered effective to reduce the seismic response of buildings. Moreover the energy dissipation capacity directly affects the response of buildings simulated with an inelastic dynamic analysis. Therefore, the precise evaluation of the energy dissipation capacity is necessary to understand the behavior of buildings under inelastic deformations.

In order to ensure sufficient energy dissipation capacity of the beam-column joint, the design guidelines of the Architectural Institute of Japan (1999) (AIJ guideline) require that the bond stress on the beam longitudinal bar passing through the joint not exceed bond resistance. The amount of joint hoops must also satisfy the minimum requirement for the same reason.

Shiohara (2009) has stated that failure of beam-column joints tends to occur as the value of column-to-beam flexural strength ratio approaches 1.0, even when the beam-column joints have some margin for joint shear capacity. This claim is based on an analytical study using new concepts on the moment capacity and balanced failure of beam-column joints which he has previously proposed (Shiohara (2008)). Kusuhara et al. (2010) have conducted experiments on 26 interior beam-column subassemblages without applying axial forces. They have indicated that specimens with column-to-beam flexural strength ratios in the range of 1.0 to 1.5 exhibit joint failure. Their hysteresis loops have a pinched shape and the energy dissipation capacity is small.

The objective of this experimental study is to investigate the energy dissipation capacity of beam-column connections, with low column-to-beam flexural strength ratio as seen in practical design, whose joint expansion is confined by joint hoops, column axial load, and column longitudinal bars. The effect of improving bond resistance of the beam longitudinal bars is also investigated.



(a) Elevation of test specimens (Note: Dimensions in mm)

	No.1	No.2	No.3	No.4	No.5	No.6	No.7
Beam				5-D16(SD390)			7+7-D10 (SD390)
Column		12-D16(SD390)		16-D16(SD390)	12-D16(SD390)		
Joint	3-D6(SD295)@100	3-D6(SD345)@40	6-D10(SD345) @40	6-D10(SD345) @40	3-D6(SD295) @90		

(b) Cross-section detail (Note: Dimensions in mm)

Figure 2.1. Geometry and reinforcement layout of test specimens (Note: Dimensions in mm)

2. EXPERIMENTAL PROGRAM

2.1. Specimens

In this experimental study, seven interior beam-column subassemblages of reinforced concrete, a half-scale, were subjected to constant axial loading and cyclic lateral loading statically. All the specimens had the same dimensions, but the arrangement of joint hoops and column and beam longitudinal bars are different. The geometry and reinforcement layout of these specimens are shown in Fig. 2.1. A constant vertical load was applied to some specimens. Each specimen was designed in detail as follows.

Specimen No. 1 was a standard specimen of this experiment. It was designed so that the ratio of flexural strength of column, M_{cu} , without axial force to that of beam, M_{bu} , was around 1.25; the ratio of shear strength of joint, V_{ju} , to shear force in joint, V_j , computed by the AIJ guideline was around 1.15; the ratio of bond resistance on beam longitudinal bars passing through the joint, τ_u , to the bond stress, τ_j , computed by the AIJ guideline was 0.75 (Minimum requirement is 1.0, however 0.8 is allowable

for practical design.); and a lateral reinforcement ratio of joint hoops, p_{jw} , was 0.2% (Minimum requirement is 0.3% in the AIJ guideline.). The equations used to compute the values of M_{cu} , M_{bu} , V_{ju} , τ_u , τ_j , and p_{jw} are as follows.

$$M_{cu} = 0.8a_t\sigma_y D + 0.5ND\left(1 - \frac{N}{bDF_c}\right) \quad (2.1)$$

$$M_{bu} = 0.9a_t\sigma_y d \quad (2.2)$$

$$V_{ju} = \kappa\phi F_j b_j D_j \quad (2.3)$$

$$V_j = T + T' - V_c = 2a_t\sigma_y - \frac{a_t\sigma_y j}{H} \frac{L}{L_b} \quad (2.4)$$

$$\tau_u = 0.7\left(1 + \frac{\sigma_0}{\sigma_B}\right)\sigma_B^{2/3} \quad (2.5)$$

$$\tau_j = \frac{(1+\gamma)\sigma_{yu} \cdot d_b}{4D} \quad (2.6)$$

$$p_{jw} = \frac{\Sigma A_{jw}}{b \cdot j_w} \quad (2.7)$$

where a_t is an area of longitudinal tension reinforcements; σ_y is a yield strength of longitudinal reinforcement; D is a height of column; N is an compressive axial force applied to column; F_c is a compressive strength of concrete; d is a distance from extreme compression fiber to centroid of longitudinal tension reinforcement; κ and ϕ are coefficients for connection type of beam-column joint ($\kappa=1$ for interior beam-column joint and $\phi=0.85$ for not having transverse beams were used here); F_j ($= 0.8 \sigma_B^{0.7}$) is a standard shear strength of a joint; σ_B is a compressive strength of concrete in MPa; b_j is an effective width of a joint (b_j is equal to the width of column in this study); D_j is a height of column; T and T' are tension forces of longitudinal tension reinforcement of beams ($= a_t \sigma_y$ in this study); j is a distance from the centroid of the compressive resultant to the centroid of the tensile resultant ($= 7 d / 8$); V_c is a shear force of column ($= 2 \times M_{bu} \times L_b / (L \times L_c)$ in this study); L is the span ($= 3,000$ mm); H is the distance between the pin support and a loading point ($= 2,000$ mm); L_b is the internal lengths of beam ($= 2,650$ mm); σ_0 is the ratio of compressive axial force to the area of column in MPa; γ is the ratio of area of beam longitudinal bars in compression to that in tension; σ_{yu} is a yield strength estimated maximum ($= \sigma_y$ in this study); d_b is a diameter of longitudinal reinforcement; ΣA_{jw} is an area of shear reinforcements; and j_w is distance between centroids of longitudinal bars in tension and compression.

Specimen No. 2 was planned to investigate the effect of vertical constraining the joint with axial force applied by external vertical loading to the top of the upper column. The dimensions, material, and bar arrangement of the No. 2 were the same as those of the No. 1, however the applied vertical loading to these specimens are only different; the No. 1 is no vertical loading applied while the No. 2 applies compressive axial force corresponding to $0.1bDF_c$.

Specimen No. 3 was planned to investigate the effect of horizontal constraining the joint with increasing joint hoops. The No. 3 was the same as the No. 1 except for the joint hoops. The No. 1 had 3 - D6(SD295A) @100 mm and the No. 3 had 6 - D10(SD345) @40 mm. The amount and strength of the joint hoops of the No. 3 was decided to balance a horizontal constraint force, R_h , computed by Eqn.

Table 2.1. Steel reinforcement properties

Reinforcement	Bar diameter, mm	Yield strength, MPa	Yield Strain, %	Ultimate strength, MPa	Modulus of elasticity, GPa
D6(SD295A)	6	359	0.396	522	184
D10(SD295A)	10	351	0.206	480	173
D10(SD345)	10	382	0.242	535	174
D10(SD390)	10	463	0.278	613	178
D16(SD390)	16	428	0.287	660	179

2.8 with the axial force applied to the No. 2.

$$R_h = \sum A_{jw} \sigma_{jy} \quad (2.8)$$

where σ_{jy} is a yield strength of lateral shear reinforcement in joint.

Specimen No. 4 was planned to be the same as the specimen No. 3 except for applying constant axial force which corresponds to that of the No. 2 so that the effect of increasing axial force and joint hoops can be evaluated comparing with the No. 3 and No. 2, respectively.

Specimen No. 5 was planned to investigate the effect of vertical constraining the joint with increasing column longitudinal bars. The No. 5 added more column longitudinal bars to the specimen No. 1. These additional bars were arranged near the center of column not to increase the flexural strength of columns much, and the amount of those was decided to balance a vertical constraint force, R_v , computed by Eqn. 2.9 with the axial force applied to the No. 2.

$$R_v = a_v \sigma_{vy} + N \quad (2.9)$$

where, a_v and σ_{vy} are area and yield strength of the additional longitudinal reinforcements, respectively.

Specimen No. 6 was planned to increase joint hoops more than the No. 4. The No. 6 had more inner joint hoops, 6 - D10(SD345) @40 mm, than the No. 4; the horizontal constraint force of the No. 6 was doubled to that of the No. 4. Moreover, the No. 6 was also compressive axial force applied as well as the No. 4.

Specimen No. 7 was planned to investigate the effect of increasing bond resistance on beam bars passing through the joint with the more and thinner beam longitudinal bars. The amount and strength of those were decided so that the flexural strength of this specimen was almost the same as that of the No. 1 and that the ratio of bond strength to stress was almost 1.0.

The concrete used for all specimens was the same. Its properties observed from the material tests under the JIS A 1108 method for compressive strength of concrete and the JIS A 1113 method for splitting tensile strength of concrete are as follows: compressive strength was 25.7 MPa (when the strain was 2,216 μ); splitting tensile strength was 2.44 MPa; and modulus of elasticity was 24.6 GPa.

The steel reinforcements D16 (SD390) for column and beam longitudinal bars, D10 (SD390) for beam longitudinal bars, D10 (SD345) for joint hoops, D10 (SD295A) for hoops, and D6 (SD295A) for stirrups and joint hoops were tested under the tensile testing method for metallic material JIS Z 2241. The observed properties are shown in Table 2.1.

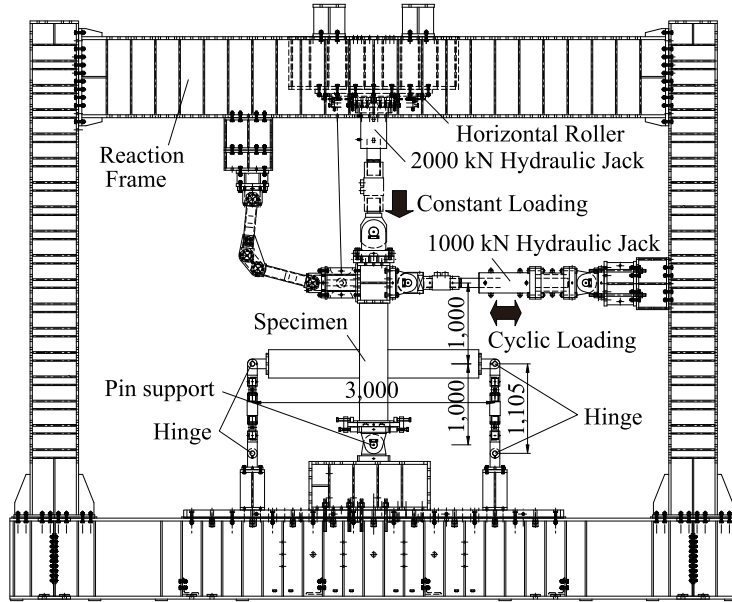
The details of all specimens computed with the observed material properties as shown above are listed in Table 2.2.

Table 2.2. Specimen details

Specimen	No.1	No.2	No.3	No.4	No.5	No.6	No.7
Beam Beam	Tensile reinforcement	5-D16 (SD390)					7+7-D10 (SD390)
	p_t , %	0.90					0.91
Column Column	Tensile reinforcement	6-D16 (SD390)			6+2-D16 (SD390)	6-D16 (SD390)	
	p_t , %	1.08			1.08*	1.08	
Beam -column joint	Lateral reinforcement	3-D6 (SD295A)		6-D10 (SD345)		6+6-D10 (SD345)	3-D6 (SD295A)
	p_{lw} , %	0.19		0.87		1.75	0.19
N , kN (η_0)		0	331 (0.1)	0	331 (0.1)	0	331 (0.1)
M_{uc} / M_{ub}		1.27	1.71	1.27	1.71	1.27	1.71
V_{ju} / V_j		1.13	1.13	1.13	1.13	1.13	1.13
τ_u / τ_j		0.63	0.69	0.63	0.69	0.63	0.69
R_h , kN		67	67	327	327	67	665
R_v , kN		0	331	0	331	340	331
							0

p_t = ratio of area of longitudinal tension reinforcement to bd . d = distance from extreme compression fiber to centroid of longitudinal tension reinforcement (= 315 mm for No. 1 - 6; 297.5 mm for No. 7). b = width of beam or column (= 350 mm). D = height of column (= 350 mm). N = axial force. η_0 = ratio of axial force to bDF_c . F_c = compressive strength of concrete. M_{cu} , M_{bu} , V_{ju} , V_j , τ_u , τ_j , p_{lw} , R_h , and R_v = shown in Eqn. 2.1 - 2.9

* The additional longitudinal reinforcements were ignored.

**Figure 2.2.** Test setup (Note: Dimensions in mm)

2.2. Loading and Measuring Programs

All specimens were supported and statically loaded as shown in Fig. 2.2. The bottom of the lower column was connected with pin support, and both beam ends were supported with horizontal rollers composed of steel rod with two hinges. Constant vertical force and cyclic lateral forces were applied to the top of the upper column with two servo-controlled hydraulic jacks. The cyclic loading was displacement controlled and gradually increasing from 2.5 mm (= 1/800 rad.) to 12 mm (= 1/17 rad.) as shown in Fig. 2.3.

The applied vertical and lateral forces were measured with load cells attached to the hydraulic jacks. At the beam ends, reaction forces were measured with load cells. Displacement transducers were set up to measure an overall lateral deflection and local deformations of beams, columns, and joint. Strains of column and beam longitudinal bars and joint hoops were measured with strain gages.

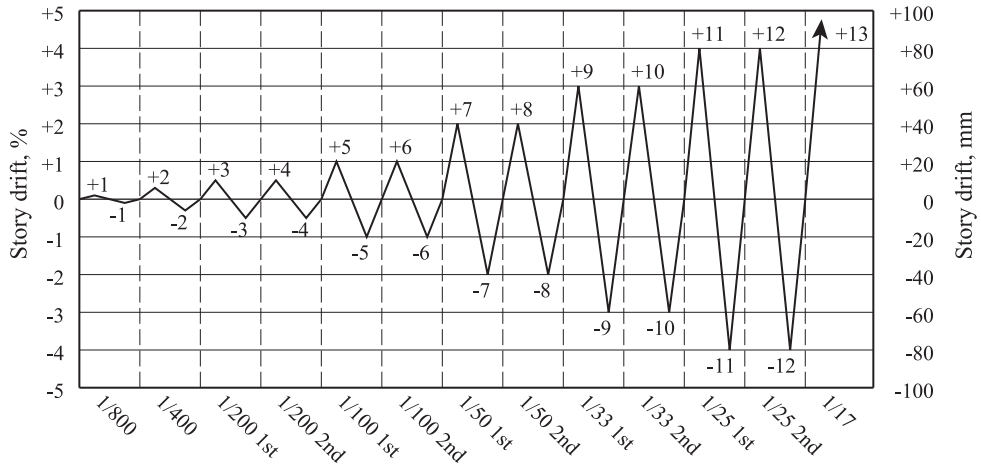


Figure 2.3. Loading procedure

3. EXPERIMENTAL RESULTS AND DISCUSSION

3.1. Overall behavior

The measured hysteresis loops for the story shear force, Q ($= P_h + P_v \delta / H$; P_h and P_v are the forces applied by the lateral and vertical hydraulic jacks, respectively; δ is the lateral displacement at loading point; and H ($= 2,000$ mm) is the distance between the pin support and the loading point.), versus the story drift angle, R ($= \delta / H$), are shown in Fig. 3.1. This figure also shows when column and beam longitudinal bars and joint hoops first yield at measured points. In addition, the story shear forces corresponding to the flexural strength of beam and shear strength of joint were indicated as Q_{bu} and Q_{ju} , respectively.

Fig. 3.2 shows typical cracking pattern of the No. 1, No. 6, and No. 7 when the story drift ratio first reached 2%, almost the same deformation reaching maximum strength, and 4%, after strength deterioration occurred. The diagonal cracking in the joint was observed in these specimens at $R = 2\%$ although flexural cracking at beam ends was relatively large in No. 6. Moreover the diagonal cracking in joint extended severely at $R = 4\%$. The similar cracking pattern was observed in the other specimens.

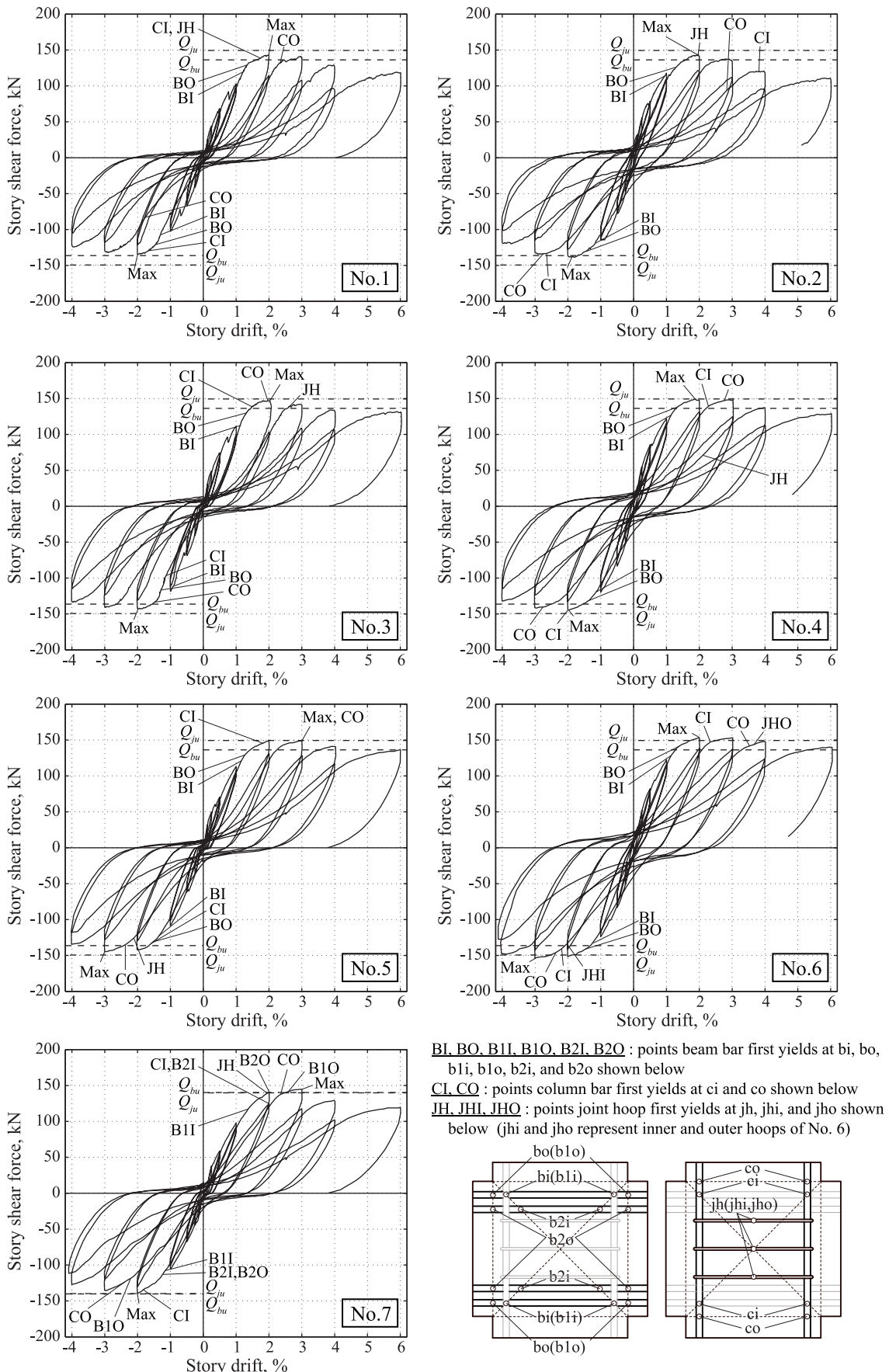
The beam longitudinal bars first yielded in joint before at column face. After that, story shear force reached maximum before column longitudinal bars yielded in the specimens axial force applied (No. 2, No. 4, and No. 6), while column longitudinal bars yielded before reaching maximum shear force in the specimens without applying axial force (No. 1, No. 3, No. 5, and No. 7). The observed maximum shear force reached Q_{bu} except the No.1 in negative loading. The shear force declined after reaching maximum strength with increasing deformation. The specimens with more joint hoops or column longitudinal bars such as the No. 3, No. 4, No. 5, and No. 6 tended to decline gently. The hysteresis loops showed a pinched shape in all specimens.

3.2. Energy dissipation

Fig. 3.3 shows equivalent damping factor h_{eq} , which was computed by Eqn. 3.1. The circle markers represented the first cycle and the square markers represented the second cycle of each drift angle.

$$h_{eq} = \frac{1}{4\pi} \frac{\Delta W}{W_e} \quad (3.1)$$

where ΔW and W_e are energy dissipations represented as the areas shown in Fig. 3.3.



BI, BO, B1I, B1O, B2I, B2O : points beam bar first yields at bi, bo,
 b1i, b1o, b2i, and b2o shown below
CI, CO : points column bar first yields at ci and co shown below
JH, JHI, JHO : points joint hoop first yields at jh, jhi, and jho shown
 below (jhi and jho represent inner and outer hoops of No. 6)

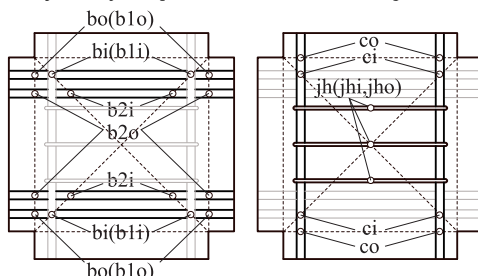


Figure 3.1. Story shear force versus story drift of specimens

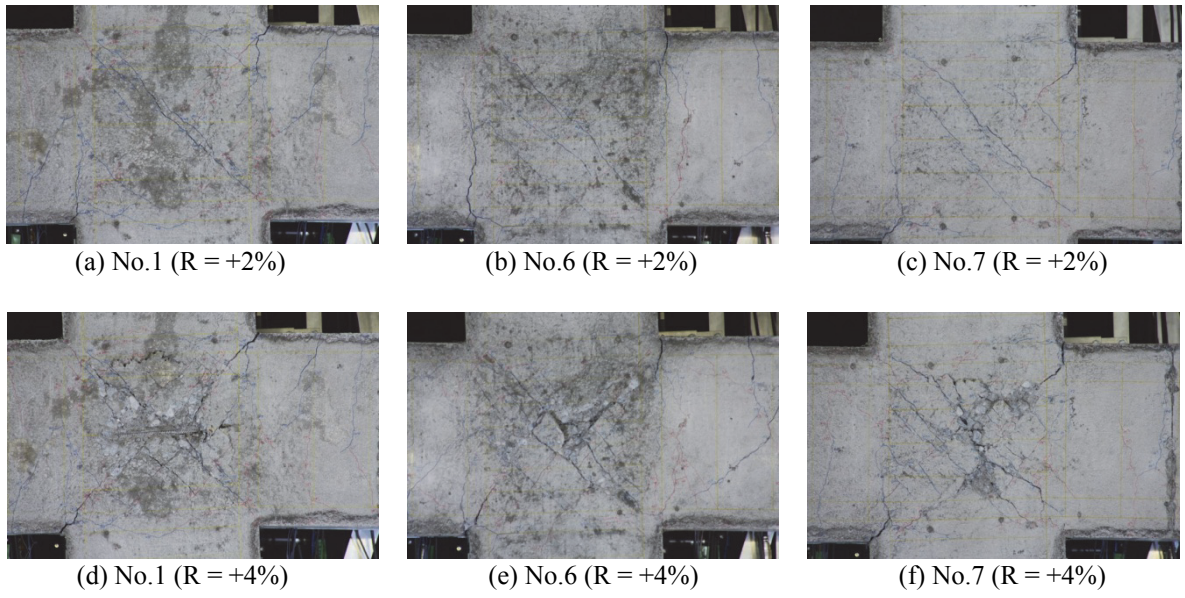


Figure 3.2. Typical cracking pattern of specimens

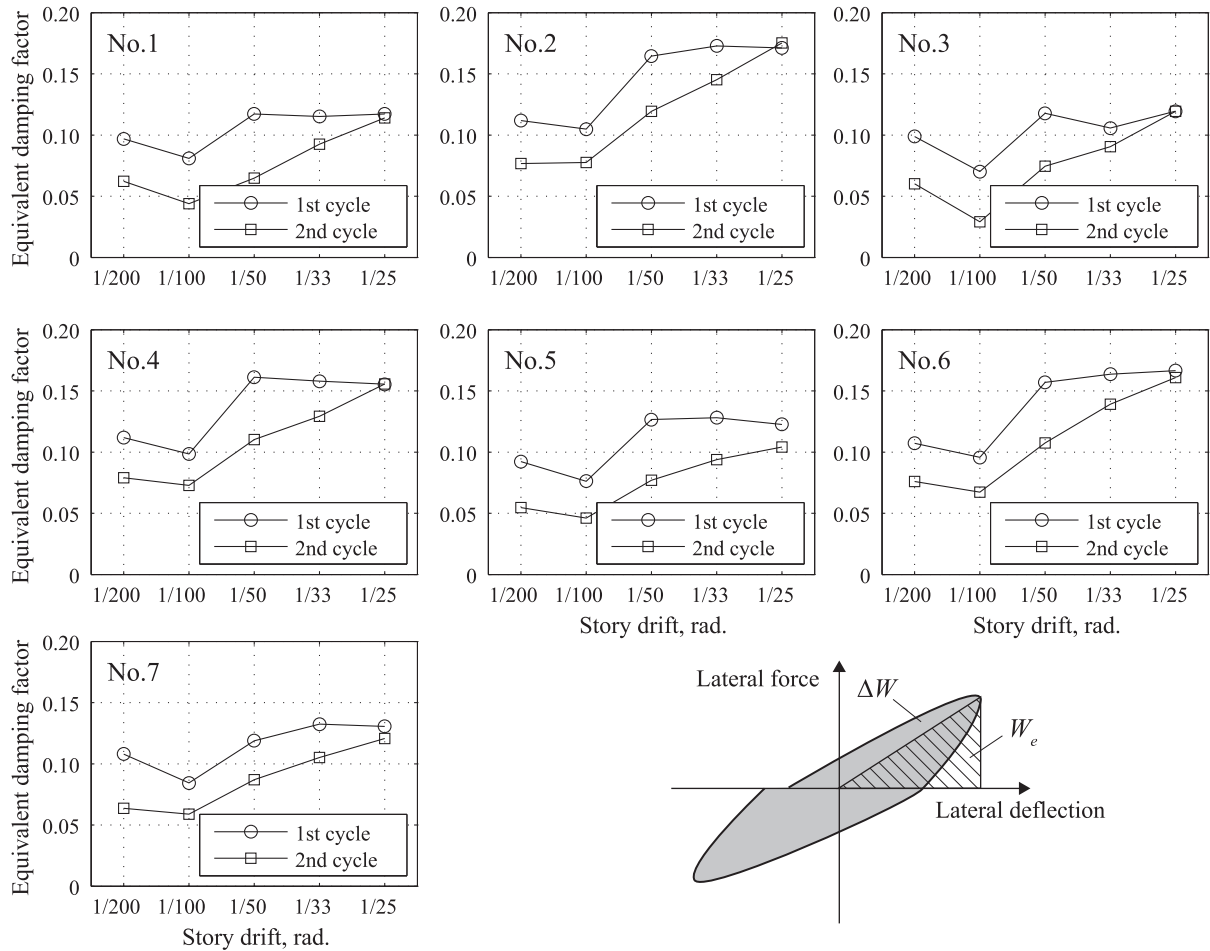


Figure 3.3. Equivalent damping factor

The equivalent damping factor in the first cycle was almost larger than that in the second cycle for all specimens. The equivalent damping factor tended to be larger when the story drift was larger.

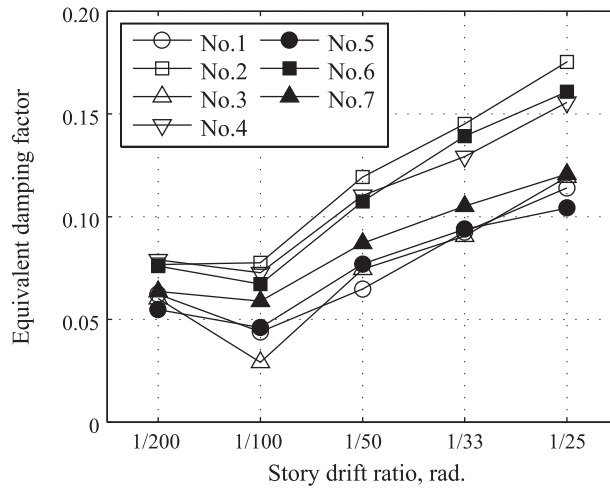


Figure 3.4 Comparison of equivalent damping factors of all specimens

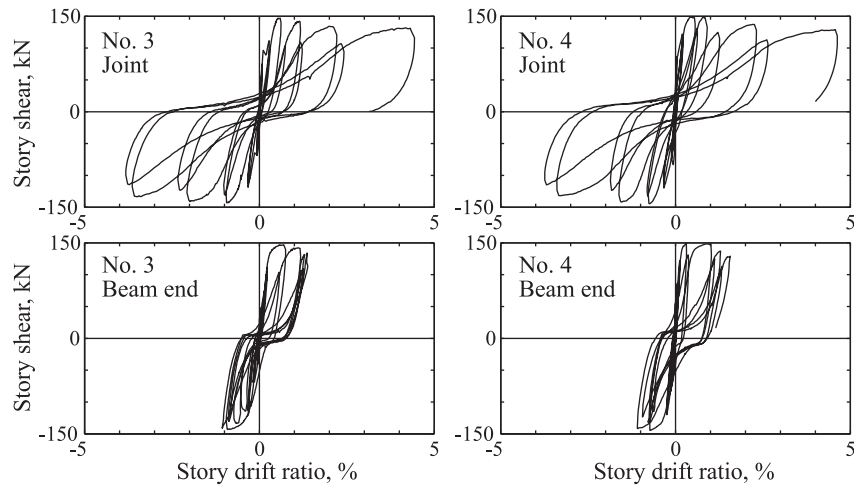


Figure 3.5 Story shear force versus story drift caused by deformation of joint and rotation at beam end

3.3. Discussions

Fig. 3.4 compares equivalent damping factors in the second cycle of each drift angle. Only the amount and yield strength of joint hoops was different between the No. 1 and No. 3 as well as among the No. 2, No. 4, and No. 6. The No. 1 and No. 3 had almost the same equivalent damping factor as well as No. 2, No. 4, and No. 6. This indicates that the amount and yield strength of joint hoops have not much to do with the equivalent damping ratio.

As for the No. 1 and No. 2, they had the same dimensions and bar arrangement, but the applied axial force was only different; the applied vertical forces of No. 1 and No. 2 were zero and 331 kN, respectively. The equivalent damping factor of the No. 1 was 0.3 - 0.5 larger than that of the No. 2. The similar relationship was shown between the No. 3 and No. 4. Fig. 3.5 shows story shear force versus story drift caused by deformation of joint and rotation at beam end. The hysteresis loops of joint were very similar, but the No. 3 dissipated more energy than the No. 4 especially in small drift. This indicated that beam-column connections with axial force have more energy dissipation than those without axial force because of increasing energy dissipation at beam end.

The No. 5, which had additional column longitudinal bars, showed almost the same energy dissipation as the No. 1. As indicated above, the energy dissipation increased with applying axial force in small deformation, while the constraint force of joint of this specimen was low in small deformation. Then,

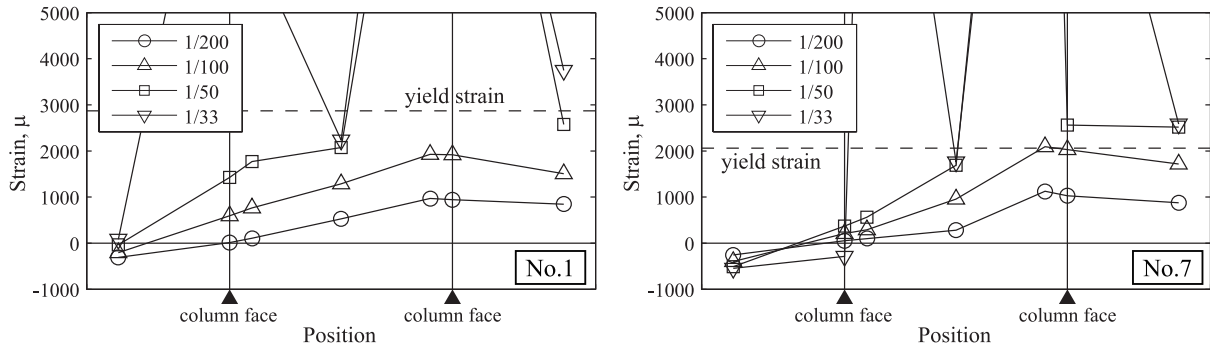


Figure 3.6 Strains of longitudinal beam bars

it is indicated that increasing column longitudinal bars for vertical constraint of joint does not improve the energy dissipation capacity.

The No. 7 had more and thinner beam longitudinal bars than the No. 1 to improve bond resistance. The No. 7 had a little larger energy dissipation capacity than the No. 1, but smaller than the No. 2, No. 4, and No. 6 which applied axial force. Fig. 3.6 showed strains of beam longitudinal bars of the No. 1 and No. 7. The both showed similar strain distribution, and bond deteriorations were not apparently shown.

4. SUMMARY AND CONCLUSIONS

This study investigated the energy dissipation capacity of reinforced concrete interior beam-column connections. Seven half-scale beam-column subassemblages whose joint expansion was confined by joint hoops, column axial load, and column longitudinal bars were tested under static cyclic loading. Based on the experimental results, the following conclusions are drawn:

- 1) Specimens confined by column axial load showed a higher energy dissipation capacity than the unconfined specimens.
- 2) The amount and yield strength of the joint hoops and column longitudinal bars had little effect on the energy dissipation capacity.
- 3) The specimen with improved bond resistance showed a slightly higher energy dissipation capacity, but not as much as the specimens confined by column axial load.

ACKNOWLEDGEMENT

The financial support of the Ministry of Land, Infrastructure, Transport and Tourism of Japan through the Project for Promoting Development of Building Standard Laws is gratefully acknowledged.

REFERENCES

- Architectural Institute of Japan. (1999). Design Guidelines for Earthquake Resistant Reinforced Concrete Buildings Based on Inelastic Displacement Concept, Architectural Institute of Japan. (in Japanese)
- Kusuhara, F., Shiohara, H., Tazaki, W., Park, S. (2010). Seismic Performance of Reinforced Concrete Interior Beam-column Joint under Low Ratio of Column to Beam Moment Capacity. Journal of Structural and Construction Engineering. **75:656**, 1873-1882. (in Japanese)
- Shiohara, H. (2008). Reinforced Concrete Beam-column Joint : Failure mechanism overlooked. Journal of Structural and Construction Engineering. **73:631**, 1641-1648. (in Japanese)
- Shiohara, H. (2009). Reinforced Concrete Beam-column Joint : Seismic Design of Joints Connecting Weak Beam and Strong Columns. Journal of Structural and Construction Engineering. **74:640**, 1145-1154. (in Japanese)